Reprinted from JOURNAL OF THE ELECTROCHEMICAL SOCIETY
Vol. 145, No. 3, March 1998
Printed in U.S.A.

Changes in the Electrochemical Behavior of Polymeric Carbon Induced by Heat-Treatment and Doping with Lithium Ions

Hossein Maleki,[a] Claudiu D. Cojocaru,[b] Christopher M. A. Brett,*[,b] Gwyn M. Jenkins,[c] and J. R. Selman*[,a]

[a]*Department of Chemical and Environmental Engineering, Illinois Institute of Technology, Chicago, Illinois 60616, USA*
[b]*Departamento de Química, Universidade de Coimbra, 3049 Coimbra, Portugal*
[c]*Center for Irradiation of Materials, Department of Physics, Alabama A&M University, Huntsville, Alabama 35762, USA*

ABSTRACT

The electrochemical properties of glassy carbon (GC) and GC doped with lithium ions (GC:Li^+) were investigated as a function of heat-treatment temperature (HTT). A phenolic resin precursor (liquid resol, $C_7H_8O_2$) was heat-treated to 650, 700, 1000, 2000, or 2500 °C to form GC. GC:Li^+ was made by dissolving 5% and 10% by weight $LiNO_3$ in resol (referred to as 5%WLDR and 10%WLDR, respectively) and following the same heat-treatment programs. Cyclic voltammetry was performed at GC electrodes in aqueous solutions of sulfuric acid and of potassium sulfate together with the electro-oxidation of potassium ferrocyanide. The hydrogen evolution potential became more negative with rising GC HTT, ranging from −1.2 V for HTT 650 °C to −2.0 V for HTT 2500 °C in both sulfuric acid and potassium sulfate solutions, while hysteresis in the voltammograms was reduced and the oxidation and reduction peaks disappeared. The standard rate constant of ferrocyanide oxidation at a polished electrode surface increased from 6 to 11 × 10^{-3} cm s^{-1} with increasing HTT. On adding lithium ions to the resol, the open-circuit potentials compared to undoped GC became less positive. In sulfuric acid, new cyclic voltammetric peaks emerged, anodic at +0.6 V and cathodic at +0.3 V vs the standard calomel electrode, indicative of alterations in the bulk structure of the GC matrix. Lithium doping the resin caused GC, upon heating, to lose 9–10% mass, lowered the degree of graphitization at HTTs below the melting points of LiOH and Li_2CO_3 (~720 °C), and enhanced graphitization once the lithium compounds melted and diffused away. X-ray photoelectron spectroscopy results confirmed that no lithium remained in the 5%WLDR samples if the HTT was 1000 °C or higher. Scanning electron microscopy showed that the pore-diameter distribution of GC:Li^+ differed from GC. Inductively coupled plasma atomic emission spectroscopy showed that the 10%WLDR samples heat-treated to 650 °C had a higher lithium-ion release rate than those undergoing HTTs to 500 and 575 °C, which identified lithium out-diffusion as the underlying mechanism of change in the permeability of GC as a function of HTT.

Introduction

Phenolic resin based glassy carbon[1] (GC) is particularly attractive as an electrode material because of its thermal stability, biocompatibility, robustness, and large potential range.[2-4] In fact, GC offers the widest potential range among the many types of carbon and other solid electrodes. In common mineral acids, the negative potential limit is ~−0.8 V vs SCE, except in HNO_3 with a limit at −0.6 V; the positive potential limit varies from +1.0 V in HCl up to +1.3 V in H_3PO_4.[5] A low residual current over a range of about ±1 V vs the standard calomel electrode (SCE) in aqueous media[4,5] and a more extended range in organic solvents means that GC is a good candidate electrode material in a variety of electrochemical applications.

However, for successful application it is desirable to understand the reasons for the extreme sensitivity and apparent irreproducibility of the rate of many redox reactions at the GC surface. These characteristics are due to its rich surface chemistry.[6] The electrochemical properties of GC depend on: (*i*) the raw precursor material and its additives (e.g., mass ratio of phenol to formaldehydes in the case of resol $C_7H_8O_2$, a liquid phenolic resin), (*ii*) the heating rate and heat-treatment temperature (HTT) used in its processing, and (*iii*) the method of pretreating the electrode surface. Widely used strategies for pretreating the electrode surface include polishing,[7-10] electrochemical activation,[10-16] ultrasonic activation,[17] and laser activation.[18-20] To our knowledge, nothing has been published in the literature concerning the effects of HTT on the electrochemical behavior of GC. Additionally, although uptake of ions into electrochemically treated GC has been investigated,[21] the effect of doping the resin precursor with metallic ions and then heat-treating to various temperatures has not been studied.

Hard-carbon electrode materials may be synthesized by carbonizing various resin precursor. The product becomes electrically conductive after heat-treatment above 500 °C. It forms a semiconductor whose bandgap decreases with increasing HTT and approaches zero for HTT 3000 °C.[22,23] The conductivity rises by many orders of magnitude, in step with the growth of characteristic peaks in the Raman spectrum.[1]

According to our basic model[1] for the carbonization of phenolic resin $(C_7H_6O)_n$, neighboring polymeric chains in the resin coalesce to form graphene ribbons; the number of delocalized electrons grows with the degree of ribbon formation and the electrical conductivity increases. A sample which is heat-treated slowly to its precarbonization stage (HTT 500 °C), is fully carbonized at 1200 °C. The material can then be heat-treated further to 3000 °C with no phase change and with little alteration in most physical properties. Defects are removed progressively with a rise in temperature, so the electrical conductivity rises significantly with HTT above 2000 °C. Heat-treatment to 2500 °C eliminates most impurities, which diffuse to the surface and volatilize.[24]

* Electrochemical Society Active Member.

Transmission electron and electron diffraction microscopy show growing crystalline sizes with a HTT rise. Figure 1 is a transmission electron micrograph of a HTT 2500 °C GC electrode material that we used in this work, recorded with a JEOL-4000EX ultrahigh-resolution transmission electron microscope. Note the distinct 002 interlayer spacings within the stacked graphene ribbons. The spacings between the ribbons are sites suitable for lithium-ion intercalation, whereas the gaps among the randomly dispersed short-range graphene ribbons provide additional sites suitable for lithium-ion adsorption. For samples heat-treated between 600 and 1200 °C, lithium-ion adsorption depends on the percentage of associated hydrogen atoms attached at the ribbon edge in such intermediate pyropolymers. These characteristics make resin-based GC (capacity near 560 mAh g^{-1})[25] a better candidate than graphite (capacity 372 mAh g^{-1}) for the high-capacity anode material needed in lithium-ion batteries for consumer electronics.

We have previously shown that the heating rate and HTT affect the mechanical, electrical, and thermal properties of GC as well as its permeability to ionic penetration, which passes through a maximum at HTT 650 °C.[1,5] We investigate the influence of HTT on electrochemical characteristics of GCs by examining their electrochemical behavior in aqueous H_2SO_4 between the solvent-decomposition potential limits, and on the rate of electro-oxidation of $Fe(CN)_6^{4-}$ in K_2SO_4 solution. The latter is widely employed for studying the electrochemical properties of different carbon electrode materials.[26-28] The main technique used in this work is cyclic voltammetry; some square-wave voltammetry and electrochemical impedance measurements of ferrocyanide oxidation were also carried out to compare results from different techniques.

The carbonization of hard carbon materials may be modified by incorporation of ions soluble in their precursors. Therefore, we also investigated the influence of lithium-ion doping on GC (GC:Li^+) heat-treated to various temperatures. Lithium was chosen because of its well-known applications in lithium-ion batteries. Samples were made by dissolving 5 and 10 wt % $LiNO_3$ in resol (termed 5% and 10%WLDR, respectively) and then heat-treating to 500, 650, 700, 1000, and 2500 °C. The 5%WLDR sample electrodes were tested using open-circuit potential (OCP) measurements and cyclic voltammetry in 0.1 M LiCl solution; this electrolyte was chosen in order to compare with earlier results using GC electrodes implanted with 150 keV lithium ion.[29]

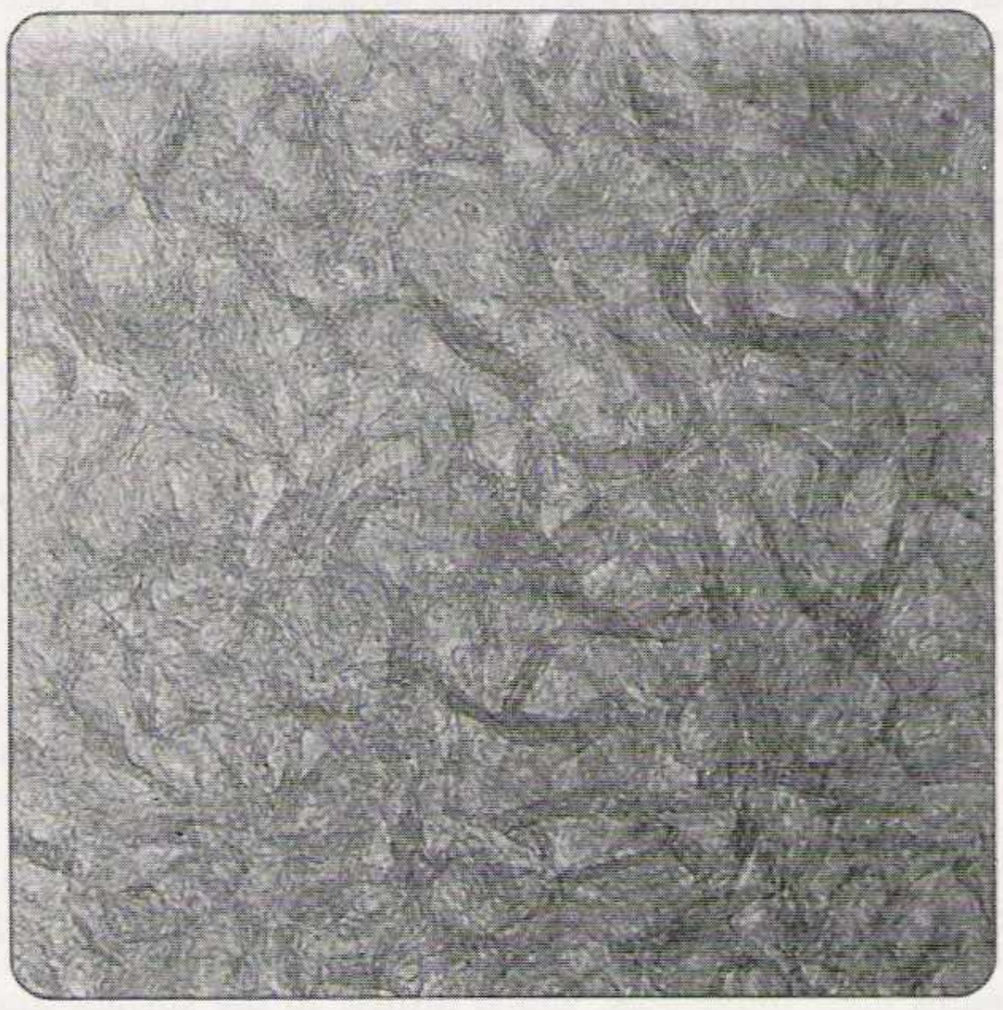

Fig. 1. Electron transmission micrograph of GC electrode material heat-treated to 2500 °C in an argon environment.

Simultaneous thermal analysis (STA) was used to determine the mass loss rate (MLR) and thermal behavior of pure resol and 5%WLDR, both cured upon heating to 1000 °C. The mass loss of 5%WLDR is about 9–10% lower than that of the pure resol, and their MLR profiles differ in the critical temperature range. This can be related to the structural differences between these samples which are reflected in their electrochemical behavior.

It is known that the porosity and permeability of GC depend on the HTT, especially between 500 and 700 °C,[24] and the nature of the starting materials. Inductively coupled plasma atomic emission spectroscopy (ICP-AES) was used to determine the lithium-ion release rate from 5%WLDR and 10%WLDR after heat-treatment to 500, 575, or 650 °C. To illustrate more clearly the HTT effects on the permeability of the GC, results for only 10%WLDR samples are presented in this work. No ICP-AES was performed on the samples heat-treated to 1000 °C and higher, since x-ray photoelectron spectroscopy (XPS) results showed them to have near-zero lithium content. XPS was used to determine the lithium content of GC:Li^+ electrode materials, prepared from cured 5%WLDR heat-treated to 500, 700, 1000, and 2500 °C. The results show that the lithium and oxygen contents of the GC decrease with rising HTT.

Experimental

Specimen preparation.—Sample disks were prepared from a resol ($C_7H_8O_2$, L no. 144d56), supplied by Georgia-Pacific Co., Atlanta, GA. Cylinders were cast in a glass tube (7 mm i.d. and 60 mm long), gelled, and cured, i.e., slowly heated to 100 °C and kept for 6 h in a vertical furnace open to air. The cured resin was sliced into pieces 2.5 mm long with a diamond saw. Representative HTTs were chosen in the range 500–2500 °C. The heating rate was 4–6 °C/h up to 700°, 20 °C/h from 700 to 1000 °C, and 40–45 °C/h from 1000 to 2500 °C.

Resol ($C_7H_8O_2$) begins to polymerize at 80–100 °C. It converts to $(C_7H_6O)_n$, a fully cured phenolic resin, near 200 °C. During further pyrolysis, continuation of the curing reactions occurs between $-CH_2OH$ and the aromatic molecules and/or a condensation reaction occurs between the hydroxyl and methylene groups, which removes water from the resin. This results in a total mass loss of 35–40% for HTT up to 1000 °C. Slow heating below the precarbonization stage (500 °C) is important. This allow the gaseous products that form during early graphene ribbon formation to diffuse and evolve from the surfaces of the samples. Otherwise, cracks appear in the sample. Optimization of the heat-treating program and its critical effect on the production of a dense and defect-free GC are discussed in detail elsewhere.[30]

Lithium-ion-doped GC samples (GC:Li^+) were prepared by adding 5 wt % lithium nitrate $LiNO_3$ (Alpha) to liquid resol (5%WLDR), setting to form resin, precarbonizing, and further heat-treating to temperatures between 500 and 2500 °C following these procedures. Samples were also prepared by adding 10 wt % $LiNO_3$ to resol (10%WLDR) and heating to 500, 575, or 650 °C. In this HTT range, the porosity and permeability of GC are known to reach maxima,[24] and so does its lithium-ion release rate.

Electrochemical experiments.—Specimen disks of GC (area 0.28 cm^2) were made into electrodes by attaching a copper wire to the rear face with silver epoxy. The assembly was sealed in a glass tube of 6 mm i.d. with regular epoxy resin to expose one face. This face was then polished to obtain a flat circular surface. Initial polishing was carried out with 600x (silicon carbide) abrasive paper followed by a diamond-sprayed polishing cloth, using successively smaller diamond particle sizes down to 1 μm until a mirror finish was obtained. Between experiments, specimens were polished with 1 μm diamond-sprayed cloth. The electrochemical cell also contained a Pt gauze counter electrode and an SCE as reference electrode.

Rectangular-sheet specimens of GC:Li^+ (made from 5%WLDR and heat-treated between 500 and 2500 °C) of area 1.5–2.5 cm^2 were made into electrodes in a similar

way as the GC disks and sealed in epoxy resin, leaving one face open for exposure to electrolyte. No polishing was done since this could influence the egress of Li^+.

An EG&G Princeton Applied Research (Princeton, NJ) 273A potentiostat/galvanostat was used with M270 Research Electrochemistry software, M271 Cool Kinetic Analysis software, and M352 Corrosion Analysis software. Some experiments were conducted with an Autolab PGSTAT10 (Ecochemie, Utrecht, Netherlands).

All solutions were made from analytical-grade reagents and Millipore Milli-Q ultrapure water (resistivity 18 MΩ cm). Electrolyte solutions were deoxygenated by bubbling oxygen-free nitrogen through the solutions for 15 min prior to, and also during, experiments. It was found that the influence of oxygen removal from the solutions on the experimental results was not significant.

Simultaneous thermal analysis (STA).—We used a Stanton-Redcroft simultaneous thermal analyzer (STA), 780 Series, at Oak Ridge National Laboratory (Metal and Ceramic Division), to determine the mass loss rates of disks of cured resol and 5%WLDR samples and determine the endo/exothermic nature of the reactions of species present during their carbonization, on heating from room temperature up to 1000 °C. The disks were 4 mm diameter, ~0.3 mm thick and of mass 18.5 ± 0.1 mg. Detailed data on mass loss effects, experimental setup and measurements technique are given elsewhere.[30] Some mass spectrometry was also carried out on pure resin while heating it to 1250 °C.

ICP-AES measurements.—Three sets of five GC:Li^+ samples (each 1.0 × 1.0 × 0.1 cm) were prepared from 10%WLDR heat-treated to 500, 575, or 650 °C, and each sample was soaked in 5 ml phosphate-buffered-saline solution (PBS, pH 7.4 at 25 °C, phosphate buffer 0.01 mol dm^{-3}, NaCl: 0.137 mol dm^{-3}, KCl: 0.0027 mol dm^{-3}). The amount of lithium ion leached from each of three sets of five samples into the PBS solution was measured every 24 h for 5 days by ICP-AES using a Perkin-Elmer Plasma 400 spectrometer. Between measurements, the samples were placed in fresh PBS solution to monitor lithium-ion release during the following 24 h.

X-ray diffraction.—The structural changes in GC:Li^+ and GC were determined from XRD profiles produced by a Philips PW-1840 powder diffractometer equipped with a copper target X-ray tube and diffracted-beam monochromator. The powder sample was packed into a 25-mm long (parallel to the beam line), 15-mm wide, and 1-mm deep sample holder. 2θ values between 5 and 120 °C were used for all samples.

Results and Discussion

Results are presented in two parts. The first part involves the electrochemical characterization of the surfaces of electrodes made from GC of various HTTs by cycling in sulfuric acid solution between the hydrogen and oxygen evolution potentials and by determining the kinetics of the oxidation of ferrocyanide. Information on surface oxygen obtained by electron microprobe analysis is included, because carbon surfaces can have species such as hydroxyl, carbonyl, carboxylate, and quinone groups, and others.[2]

The second set of results concerns the effect that lithium-ion doping of the resin precursor has on the electrochemical behavior of GC in LiCl solution. This electrolyte is used in order to prevent significant egress of lithium from the electrode during experiments. Results of differential thermogravimetry and differential scanning calorimetry (DSC) are included to show that the mechanism of mass loss is different for GC:Li^+ and GC, and most likely this is the key to their different electrochemical behavior.

Electrochemical characterization of GC electrodes.—Cyclic voltammetry in sulfuric acid solution.—Cyclic voltammograms (CVs) obtained in 0.5 M H_2SO_4 at carbonized resin electrodes between −2.0 V vs SCE are shown in Fig. 2. These voltammograms were obtained in nondeaerated solution; however, deoxygenation led to no visible difference in the voltammograms. A large hysteresis is observed in the cathodic part of the voltammetric curves for the 650 and 1000 °C electrodes. This hysteresis disappears for the 2500 °C electrode. In particular, for the two lower HTT samples, a large cathodic peak was found around −1.2 V which must be due to the reduction of protons close to the surface (see next section). The oxygen evolution potential remained at about +2.0 V, with a slight tendency to become less positive with increasing HTT. As the HTT of the samples increased, small voltammetric peaks for reduction and oxidation of surface species were found to develop at −0.5 and +1.5 V, respectively. Additionally, on second and subsequent cycles a small peak emerged at +0.3 V.

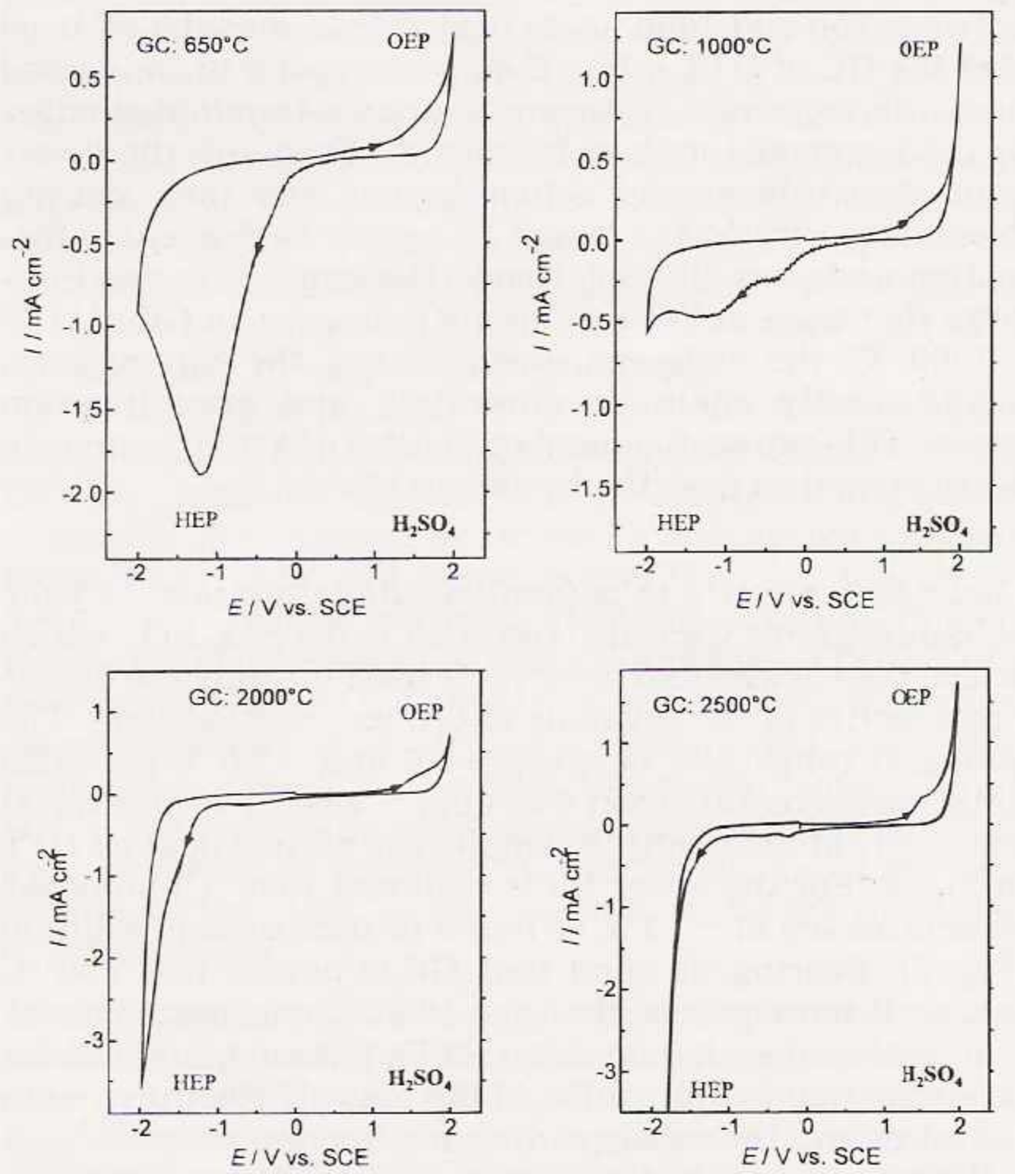

Fig. 2. Cyclic voltammograms in 0.5 M H_2SO_4 electrolyte at GC as a function of electrode HTT. Potential range ±2.0 V vs SCE; scan rate 50 mV s^{-1}.

In order to investigate further the nature of these peaks, cyclic voltammograms were recorded while reversing the positive-going potential scan at +1.5 V, i.e., before oxygen evolution: a small voltammetric peak at −0.5 V persisted. Cyclic voltammograms were also recorded with potential limits of +1.0 and −1.0 V (not shown). The cathodic peak disappeared and only small currents were measured which decreased slightly with increasing HTT, down to 30 μA cm^{-2} for HTT 2000 °C and above. The response was independent of the solution being deoxygenated or not, suggesting that the peaks observed are due to surface-confined species.

Similar cyclic voltammograms have been observed by other authors in sulfuric acid solution[31] and in the context of a study on the influence of pH on the electrochemical response of carbon electrodes.[32] No exact identification of the peaks was made but the formation and reaction of a graphitic oxide film which undergoes oxidation and reduction was invoked. A similar type of explanation is appropriate here, particularly given the symmetric shape of the cathodic peak.

The changes in surface electrochemistry with HTT evidenced by these measurements correlate with the amount of residual hydrogen in the carbonized resin shown by other characterization techniques.[1] It has been demonstrated that a decrease in hydrogen content of the phenolic resin causes a marked increase in electrical conductiv-

ity (by 10^5 to 10^6 S cm^{-1}) of GC produced by heating between 650 and 1000 °C. In principle, it must be realized that the GC of HTT < 700 °C consists mostly of condensed aromatic molecules featuring hydrogen-terminated edges in the hexagonal carbon fragments. These are the dominant electrochemically active regions and their density depends mostly on the extent of carbon-carbon chain formation and cross-linking. Hence, the large hysteresis indicates that these active regions are extensive. In GC of HTT > 1000 °C, the hydrogen is eliminated, the carbon fragments mostly chain or cross-link, and graphitization grows. This causes the number density of active regions to decrease and so does the hysteresis effect.

Cyclic voltammetry in potassium sulfate solution.—Cyclic voltammograms were also recorded in 0.4 M K_2SO_4, which is also the background electrolyte used to study the oxidation kinetics of ferrocyanide at GC (see next section). The potential range was between +2.0 and −2.0 V (vs SCE) until the current reached 4 mA cm^{-2}, when sweep reversal occurred automatically. Examples are plotted against HTT in Fig. 3. For the lower HTTs (650 and 1000 °C) no peaks were observed at −1.2 V, as found in sulfuric acid solution (Fig. 2). Bearing in mind that GC is porous (the 650 °C sample is more porous than the 1000 °C one, since porosity diminished with increasing HTT), this suggests that the peaks are due to absorption of the low-pH electrolyte into the pores and the subsequent reduction of protons.

With respect to the two highest HTTs (2000 and 2500 °C), there are two main differences between Fig. 2 and Fig. 3. First, in K_2SO_4 solution oxygen evolution is greater and hydrogen evolution less than in H_2SO_4 within the potential range −2.0 to +2.0 V, as would be expected from pH considerations. Second, the reduction peak at −0.5 V, which is very small in H_2SO_4, is more pronounced in K_2SO_4 solution. This peak became about 50% larger in a cyclic voltammogram recorded after several hours immersion in aerated electrolyte, which suggests that it is due to reduction of oxygen-containing groups on the surface. Following the same procedure in deaerated solution, the increase in the size of this peak is approximately 15% smaller.

Potassium ferrocyanide oxidation.—The anodic oxidation of potassium ferrocyanide [1 mM $K_4Fe(CN)_6$ in 0.4 M K_2SO_4] was examined by cyclic and square-wave voltammetry, since the rate of this reaction at GC electrodes is known to depend on the state of its surface.[26-28] In particular, as described in the Introduction, a freshly exposed or pretreated carbon surface (using electrochemical treatment or laser activation, etc.) gives higher standard rate constants than untreated electrodes which are covered by groups such as carbonyl, hydroxyl, quinone, and carboxylate.

Cyclic voltammetry of ferrocyanide oxidation was carried out using electrodes of various HTT; some CVs at GC of HTT 650 °C are shown in Fig. 4 at a scan rate of 500 mV s^{-1}. These CVs illustrate how the ferrocyanide kinetics improve with increasing immersion period in the electrolyte. The peak current was found to be linear with the square root of the scan rate for electrodes of all HTTs at low scan rates, for example, see Fig. 5. The negative deviation at higher scan rates is due to a transition from reversible to irreversible behavior.

Values for the standard rate constant, k_0, the anodic charge-transfer coefficient, α_a, and the half-wave potential, $E_{1/2}$, were determined by fitting experimental voltammograms recorded after 30 min immersion. The Cool algorithm[33,34] was used after background subtraction. The results are given in Table I for the lowest and highest HTT

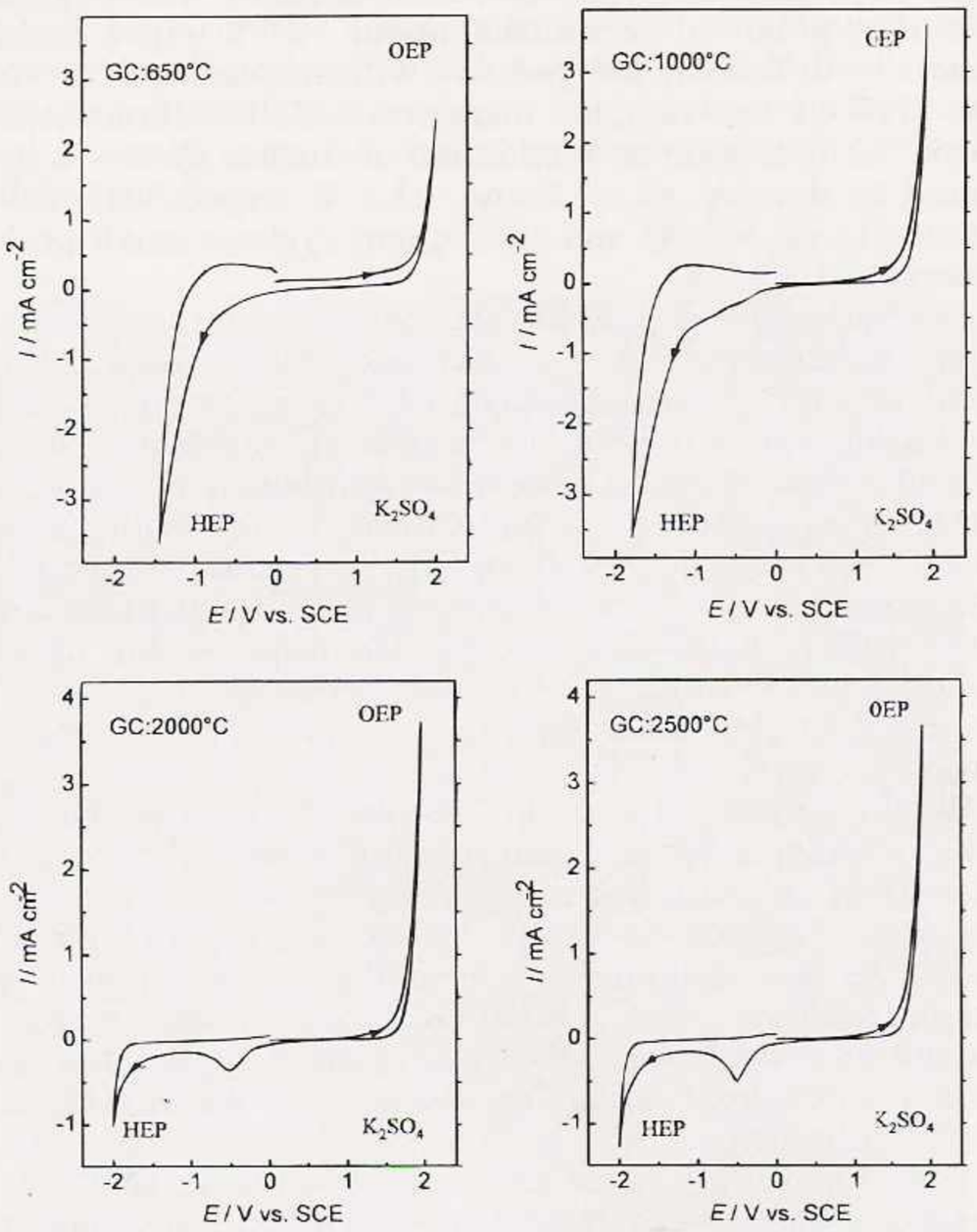

Fig. 3. Cyclic voltammograms in 0.4 M K_2SO_4 electrolyte at GC electrodes as a function of electrode HTT. Potential range ±2 V vs SCE; scan rate 50 mV s^{-1}.

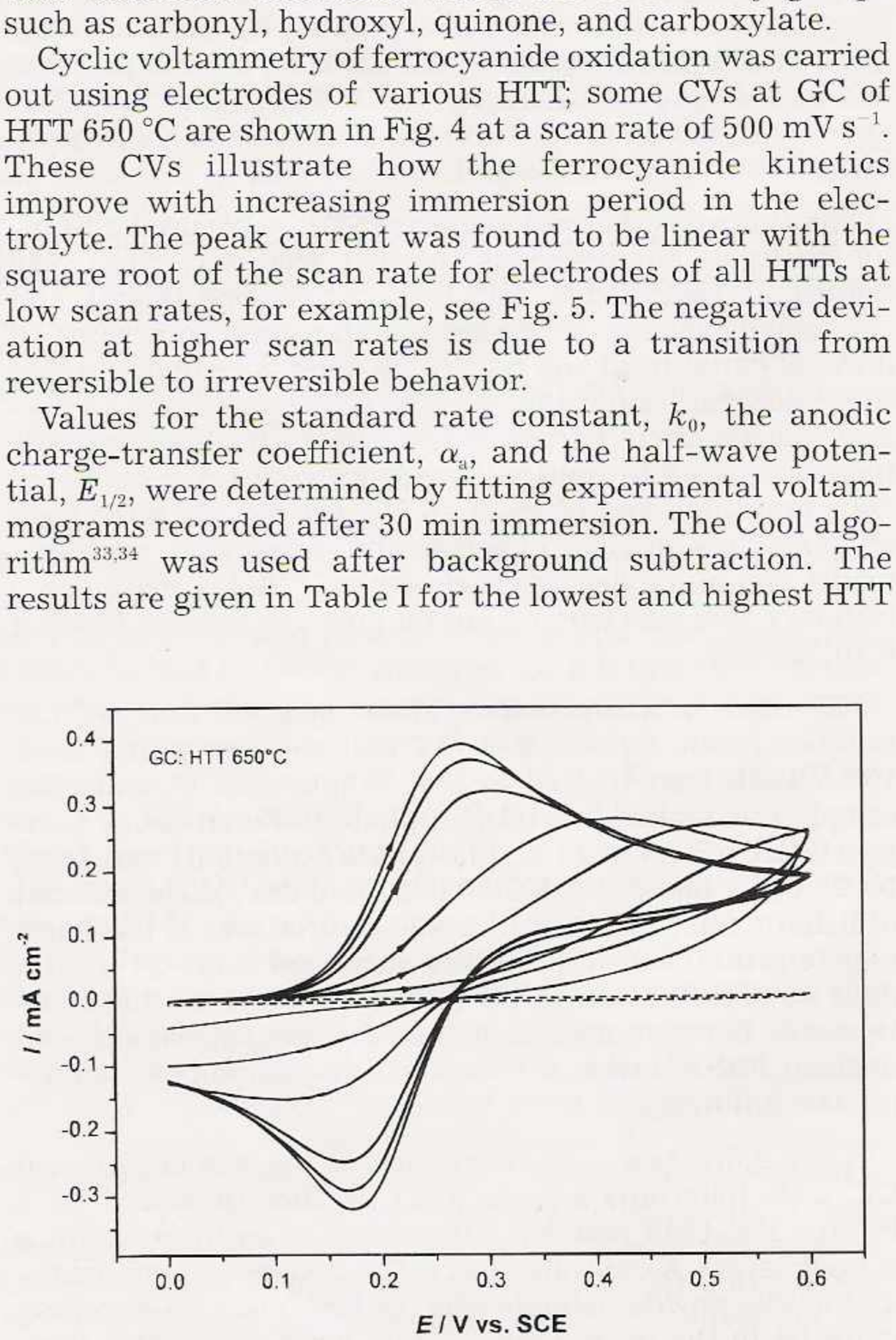

Fig. 4. Cyclic voltammograms in 0.4 M K_2SO_4 electrolyte with 2 mM $K_4Fe(CN)_6$ at GC electrode HTT 650 °C, scan rate 500 mV s^{-1}. Measurements made every hour. Reversibility increases with time. Dashed line shows initial scan in background electrolyte.

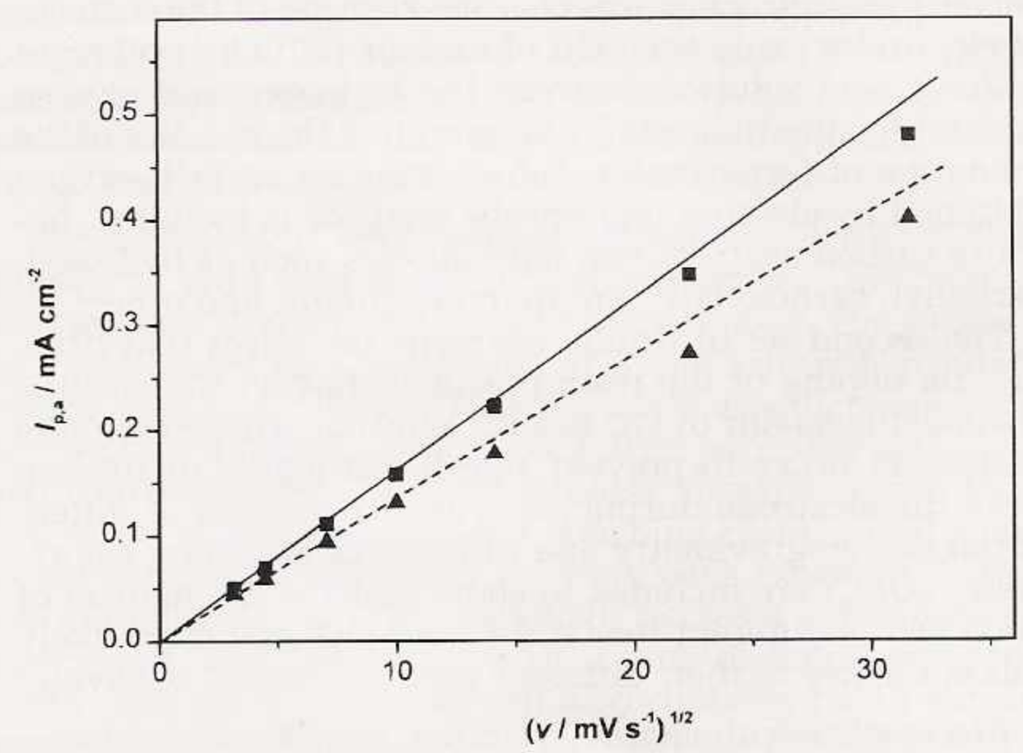

Fig. 5. Plot of anodic peak current, $I_{p,a}$, vs $v^{1/2}$ from cyclic voltammograms in 0.4 M K_2SO_4 electrolyte with 2 mM $K_4Fe(CN)_6$ at GC electrode HTT (▲) 650 and (■) 2000 °C after 2 h immersion.

ity (by 10^5 to 10^6 S cm^{-1}) of GC produced by heating between 650 and 1000 °C. In principle, it must be realized that the GC of HTT < 700 °C consists mostly of condensed aromatic molecules featuring hydrogen-terminated edges in the hexagonal carbon fragments. These are the dominant electrochemically active regions and their density depends mostly on the extent of carbon-carbon chain formation and cross-linking. Hence, the large hysteresis indicates that these active regions are extensive. In GC of HTT > 1000 °C, the hydrogen is eliminated, the carbon fragments mostly chain or cross-link, and graphitization grows. This causes the number density of active regions to decrease and so does the hysteresis effect.

Cyclic voltammetry in potassium sulfate solution.—Cyclic voltammograms were also recorded in 0.4 M K_2SO_4, which is also the background electrolyte used to study the oxidation kinetics of ferrocyanide at GC (see next section). The potential range was between +2.0 and −2.0 V (vs SCE) until the current reached 4 mA cm^{-2}, when sweep reversal occurred automatically. Examples are plotted against HTT in Fig. 3. For the lower HTTs (650 and 1000 °C) no peaks were observed at −1.2 V, as found in sulfuric acid solution (Fig. 2). Bearing in mind that GC is porous (the 650 °C sample is more porous than the 1000 °C one, since porosity diminished with increasing HTT), this suggests that the peaks are due to absorption of the low-pH electrolyte into the pores and the subsequent reduction of protons.

With respect to the two highest HTTs (2000 and 2500 °C), there are two main differences between Fig. 2 and Fig. 3. First, in K_2SO_4 solution oxygen evolution is greater and hydrogen evolution less than in H_2SO_4 within the potential range −2.0 to +2.0 V, as would be expected from pH considerations. Second, the reduction peak at −0.5 V, which is very small in H_2SO_4, is more pronounced in K_2SO_4 solution. This peak became about 50% larger in a cyclic voltammogram recorded after several hours immersion in aerated electrolyte, which suggests that it is due to reduction of oxygen-containing groups on the surface. Following the same procedure in deaerated solution, the increase in the size of this peak is approximately 15% smaller.

Potassium ferrocyanide oxidation.—The anodic oxidation of potassium ferrocyanide [1 mM $K_4Fe(CN)_6$ in 0.4 M K_2SO_4] was examined by cyclic and square-wave voltammetry, since the rate of this reaction at GC electrodes is known to depend on the state of its surface.[26-28] In particular, as described in the Introduction, a freshly exposed or pretreated carbon surface (using electrochemical treatment or laser activation, etc.) gives higher standard rate constants than untreated electrodes which are covered by groups such as carbonyl, hydroxyl, quinone, and carboxylate.

Cyclic voltammetry of ferrocyanide oxidation was carried out using electrodes of various HTT; some CVs at GC of HTT 650 °C are shown in Fig. 4 at a scan rate of 500 mV s^{-1}. These CVs illustrate how the ferrocyanide kinetics improve with increasing immersion period in the electrolyte. The peak current was found to be linear with the square root of the scan rate for electrodes of all HTTs at low scan rates, for example, see Fig. 5. The negative deviation at higher scan rates is due to a transition from reversible to irreversible behavior.

Values for the standard rate constant, k_0, the anodic charge-transfer coefficient, α_a, and the half-wave potential, $E_{1/2}$, were determined by fitting experimental voltammograms recorded after 30 min immersion. The Cool algorithm[33,34] was used after background subtraction. The results are given in Table I for the lowest and highest HTT

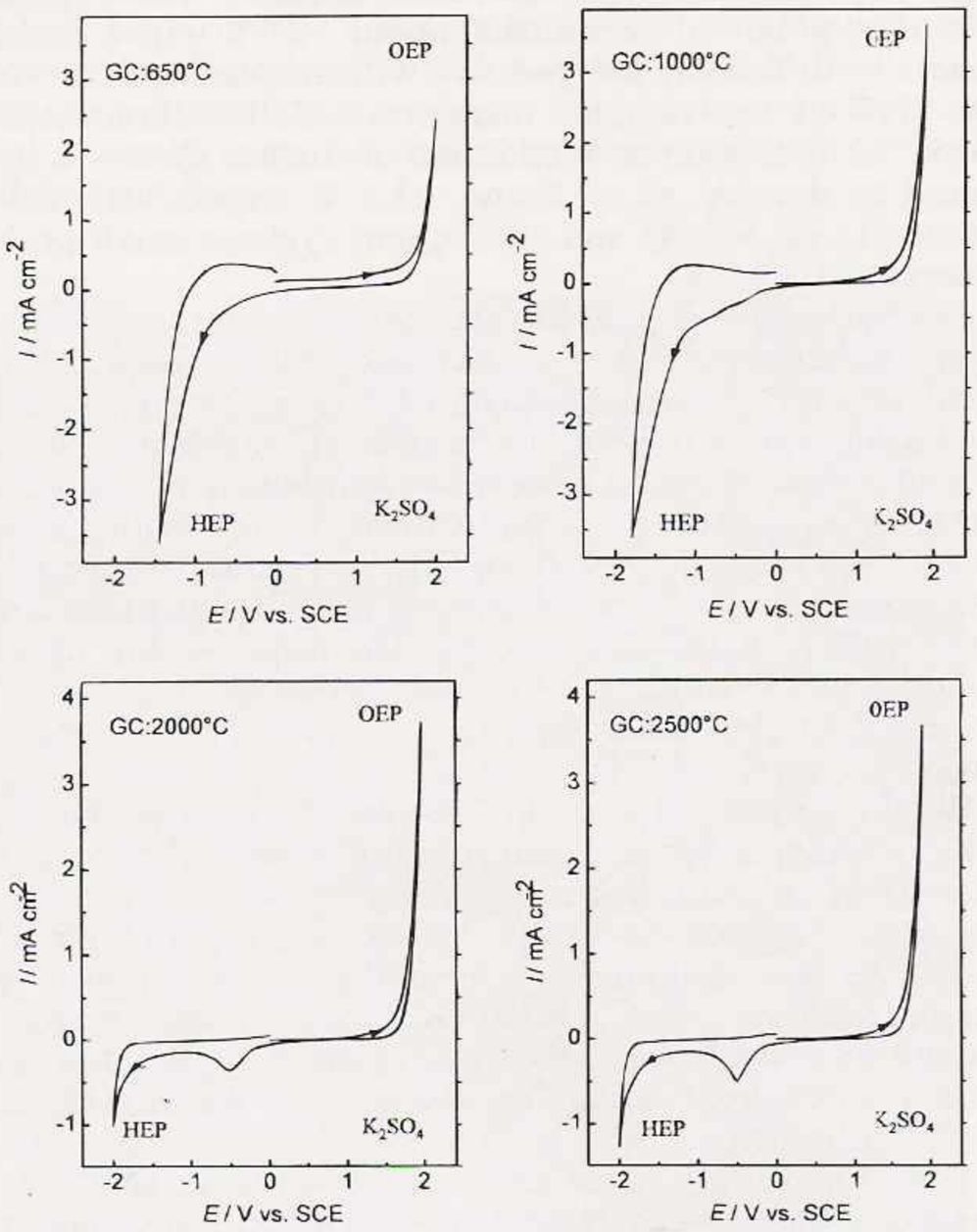

Fig. 3. Cyclic voltammograms in 0.4 M K_2SO_4 electrolyte at GC electrodes as a function of electrode HTT. Potential range ±2 V vs SCE; scan rate 50 mV s^{-1}.

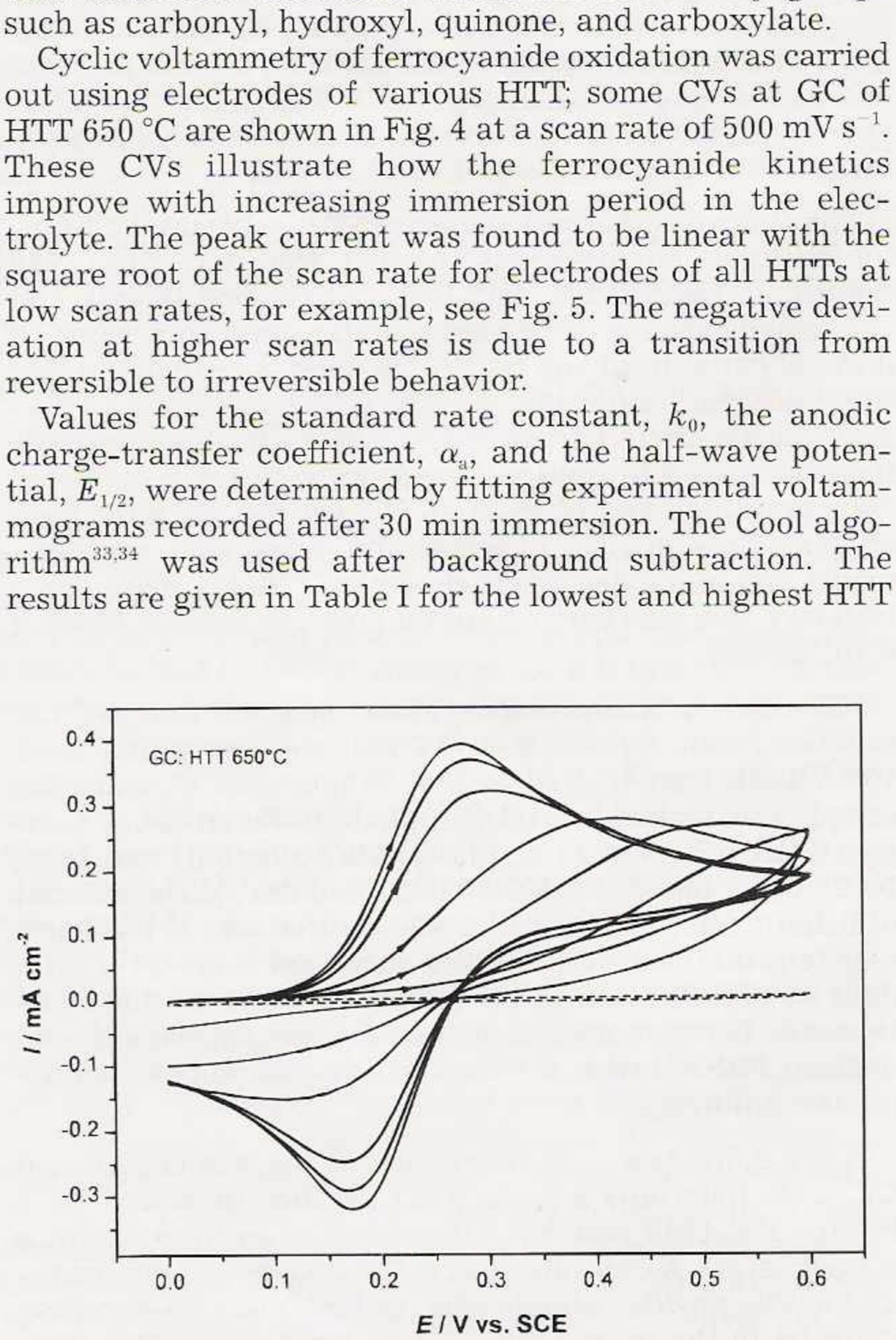

Fig. 4. Cyclic voltammograms in 0.4 M K_2SO_4 electrolyte with 2 mM $K_4Fe(CN)_6$ at GC electrode HTT 650 °C, scan rate 500 mV s^{-1}. Measurements made every hour. Reversibility increases with time. Dashed line shows initial scan in background electrolyte.

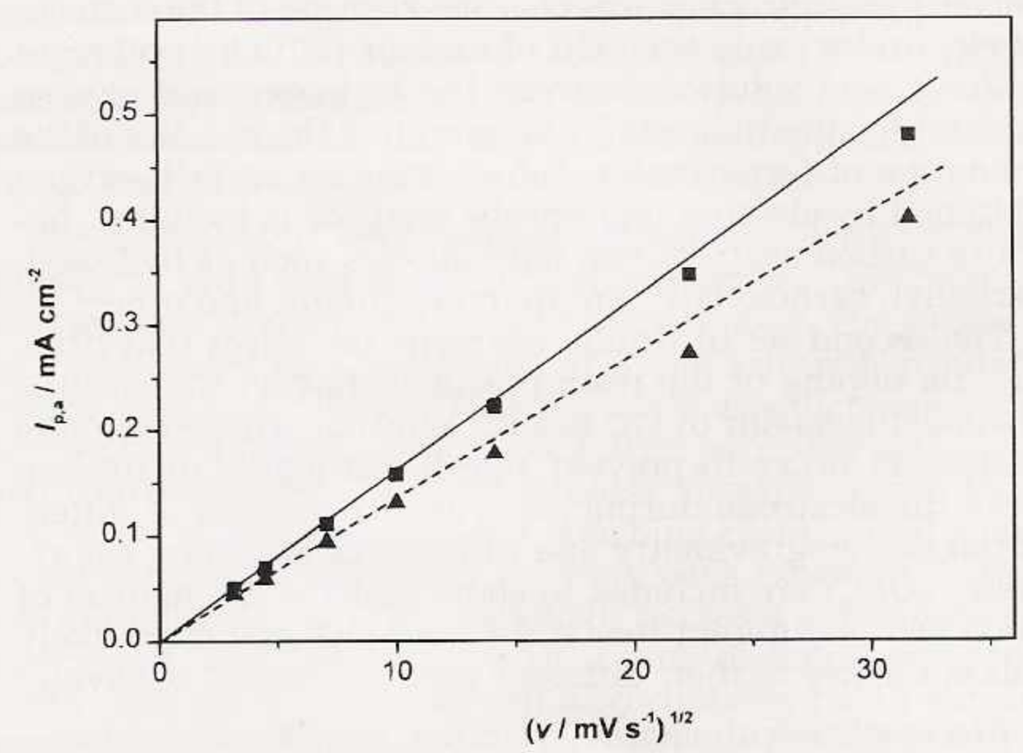

Fig. 5. Plot of anodic peak current, $I_{p,a}$, vs $v^{1/2}$ from cyclic voltammograms in 0.4 M K_2SO_4 electrolyte with 2 mM $K_4Fe(CN)_6$ at GC electrode HTT (▲) 650 and (■) 2000 °C after 2 h immersion.

700, and 1000 °C. For a HTT of 2500 °C, the ratio decreased to near zero, below the instrument sensitivity.

These results demonstrate that oxygen is intrinsically present in the as-prepared low-HTT samples and that it is present in the bulk as well as on the surface. Additionally, aging in ferrocyanide-containing electrolyte, which improves the kinetics of ferrocyanide oxidation (see Fig. 4 for example), also increases the oxygen-to-carbon ratio. The implication is that the presence of oxygen-containing groups on the carbon surface is beneficial, in this case, for increasing the rate of reaction. This is in accordance with observations made previously where oxygen-containing surface functional groups, such as carbonyl and quinone, were found to increase the kinetics of ferrocyanide oxidation through action as redox mediators, for example.[37,38]

The Effect of Doping GC with Lithium Ions

OCP in lithium chloride.—Lithium-ion-doped GC (GC:Li^+) electrodes were studied in LiCl solution in order to minimize any loss of lithium ions during the experiments and to permit an easier comparison with ref 29, which deals with lithium-ion-implanted GCs (LIGCs). Figure 7 shows the initial variation of OCP with time for both HTT 600 °C and HTT 2500 °C GC:Li^+ electrodes and that of the corresponding undoped electrodes. Significant differences are evident. The OCP of GC:Li^+ is always more negative than that of undoped GC, and the HTT affects the OCP values. The greatest influence of lithium-ion doping is on electrodes prepared from GC at HTT 600–700 °C.

Table II summarizes OCPs for GC:Li^+ after 1 and 15 h of immersion in electrolyte. The OCP remains close to zero volts vs SCE, with a tendency to become more negative with increasing immersion time and to become more positive with increasing HTT. Compared with LIGC electrodes[29] the values are more positive. As in that case, there is no suggestion of a particular potential-determining reaction but rather oxidation and reduction phenomena at the electrode surface; however, the observed potential is

Table II. OCP for Li^+-impregnated GC electrodes in 0.1 M LiCl.

	OCP (mV vs SCE)	
Pyrolysis temperature (°C)	1 h	15 h
500	12	−4
600	21	46
700	31	18
1000	92	79
2000	83	46
2500	24	9

the result of the balance between these. The negative tendency with time can be explained through the rate of surface oxidation slowing down as the surface changes toward a more stable structure. The more positive OCP values obtained at higher HTT are probably due to changes in the GC structure and greater difficulty of surface oxidation; such oxidation occurs at a higher potential, as found in the undoped material. These results are discussed further in the context of DTG and DSC studies, and some correlations are made where possible.

Cyclic voltammetry in sulfuric acid solution.—Figure 8 shows cyclic voltammograms in 0.1 M H_2SO_4 for GC:Li^+ of HTT between 500 and 2500 °C. A characteristic reduction peak at +0.3 V and an oxidation peak at +0.6 V are observed, which are not present in the undoped material. This occurs even for samples heat-treated to 2000 °C, although most of the lithium ions have diffused to the surface and evaporated off at lower temperatures. Extending the negative potential limit to more negative values (not shown) produces some noisy hydrogen evolution in the HTT 500 °C sample, indicative of a bulk reaction.

These results suggest that lithium has altered the structure and associated electrochemistry of the carbonized product through bulk chemical reactions, especially in pyropolymers heat-treated below 700 °C. The reason for this is the egress of the compounds which are formed by the reaction of lithium with the resin's by-products produced in the stages before and after the beginning of the carbonization stage (HTT ~600 °C), upon heating to 1000 °C. As compared to pure GC, they have a different open structure (see also the following section). This behavior is completely different from that observed with LIGC.[29] The effect in that case was to increase the potential range between hydrogen and oxygen evolution.

Thermal Studies on Structural Changes

Differential thermogravimetry.—We have shown previously that structure and electrical conductivity of GC can be affected by the presence of lithium.[22] The changes in

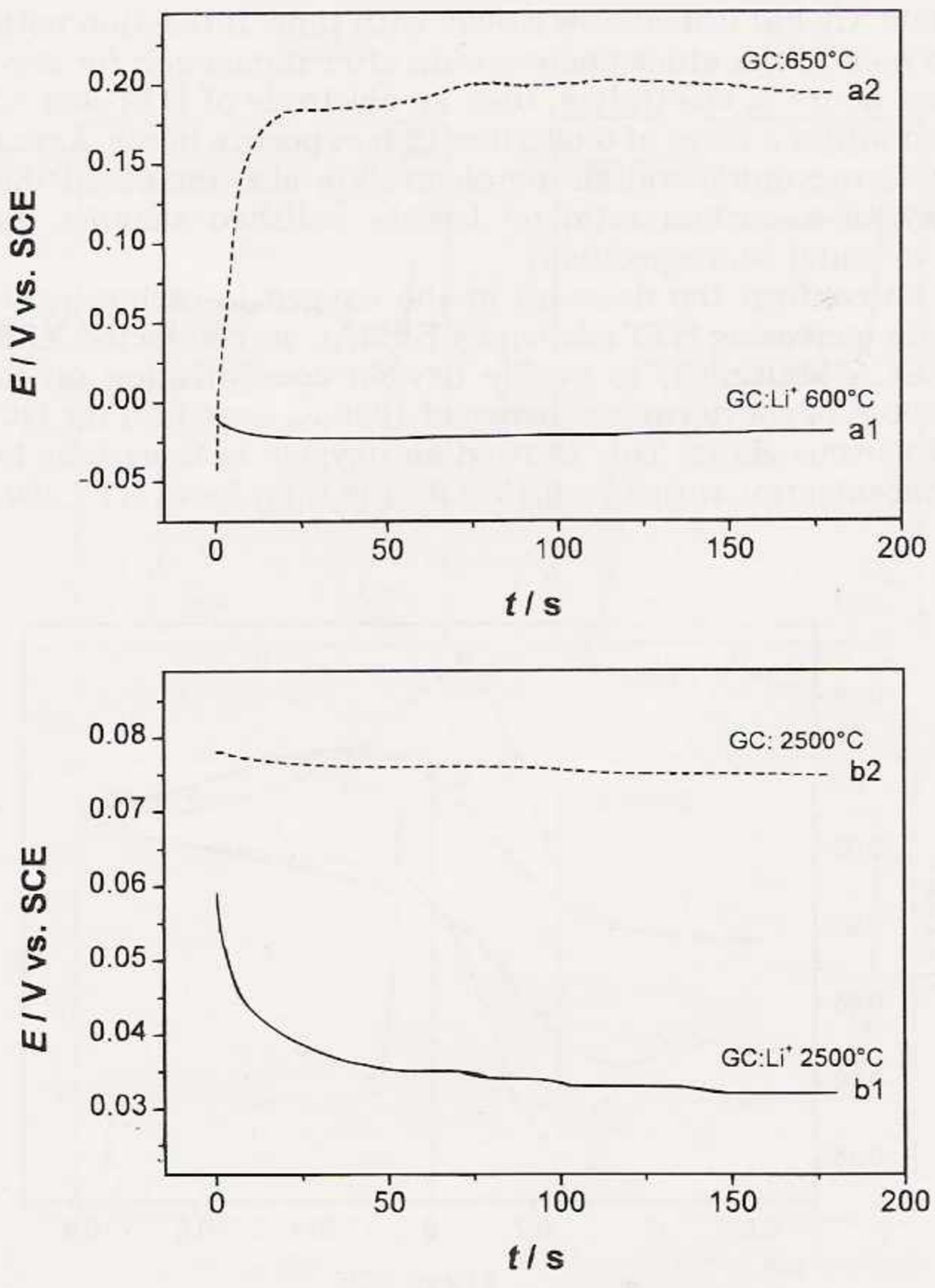

Fig. 7. Variation of OCP with time in 0.1 M LiCl for (a1) CC:Li^+ HTT 600 °C, (a2) undoped GC HTT 650 °C, (b1) GC:Li^+ HTT 2500 °C, and (b2) undoped GC HTT 2500 °C.

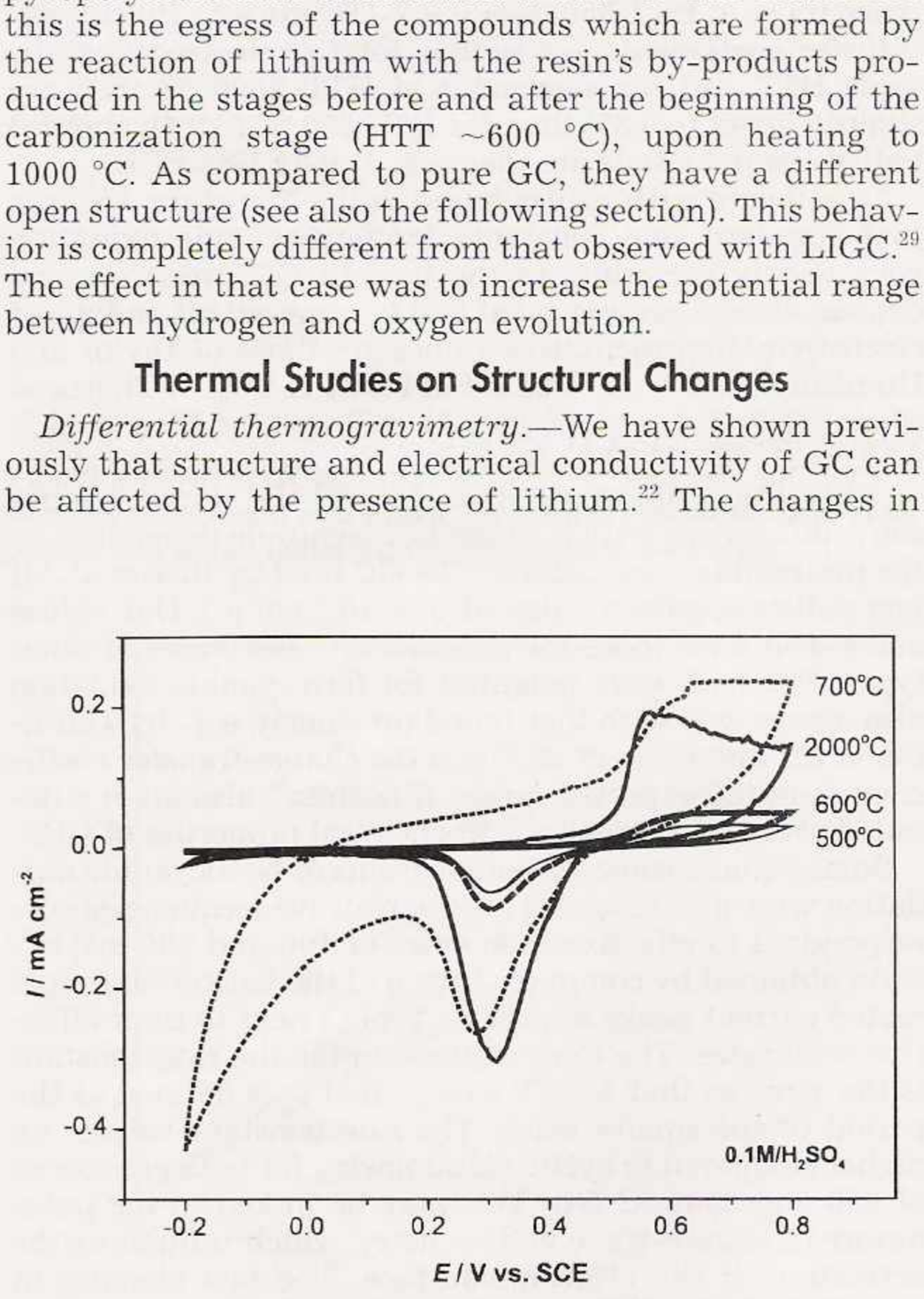

Fig. 8. Cyclic voltammograms in 0.1 M H_2SO_4 electrolyte, scan rate 50 mV s^{-1}, of GC:Li^+ sheet electrodes heat-treated to between 500 and 2500 °C.

structure of GC, doped or undoped, depend on the raw materials and the heating program.[1] These affect the chemical reaction rate of species and their gaseous products, the mass loss, and consequently, the structure of the carbonized resin product. Xiang et al.[39] used thermogravimetry (TG)/DTG experiments to show that the ratio of formaldehyde to phenol affects the mass loss of phenolic resin upon heating to 1000 °C. They related the mass loss to the carbon-carbon cross-linking density and noted that a mole ratio of 2 produces GC with the highest cross-linking density (1.294×10^3 kg/m^3). For pure resin, Yamashita and Ouchi[40] have suggested that the weight loss below 400 °C is a dewatering reaction. This is a continuation of the curing reaction between $-CH_2OH$ and aromatic hydrogen, and/or a condensation reaction between the hydroxyl and methylene groups.

In this work, we carried out TG/DTG and DSC experiments in order to probe the structural changes related to the MLRs and MS measurements to determine the nature of volatilized products upon heat-treatment of the resin samples to 1000 °C. The MS results show two high outgassing regions: one between 200 and 500 °C with a maximum ~265 °C, the principal gases being H_2O, CH_4, CH_3OH, and aromatic gas with $m/e = 29$, and another between 400 and ~630 °C with maximum ~535 °C, the gases being mostly H_2O, CH_4, CH_2, CO_2, and O_2. Hydrogen evolution was observed throughout the heating range. Our TG/DTG results correlate with regions of high MLRs which Xiang et al.[39] detected.

Figure 9 shows the MLRs obtained by DTG for 5%WLDR and pure resol, both previously cured, from room temperature to 1000 °C at 20 °C/min. The high MLR region of 5%WLDR begins near 330 °C; for resol, it begins near 420 °C and reaches a maximum at around 550 °C. The overall mass loss of 5%WLDR is less than that of resol by 9–10%. A lower mass loss simply means a higher carbon content, which can be related to a greater amount of short-range carbon-carbon chain formation and some cross-linking at temperatures lower than 700 °C, and a high degree of graphitization at temperatures ~1000 °C and higher.

The differences in the MLR vs temperature profiles of GC and GC:Li^+ in Fig. 9 also suggest that the gaseous products formed up to 600 °C diffuse to the sample surface by different mechanisms due to their different structures. Compared to 5%WLDR, the initial critical MLR for GC is delayed, and in the second region (HTT 480–600 °C) it is much larger. This suggests that the addition of $LiNO_3$ suppresses the out-diffusion of gaseous products from the resin matrix and thereby causes changes in the structure. Near and above HTTs of 650 °C, the MLRs of doped and undoped samples are closely matched. Hence lithium-ion doping mainly affects the GC structure at temperatures lower than 650 °C.

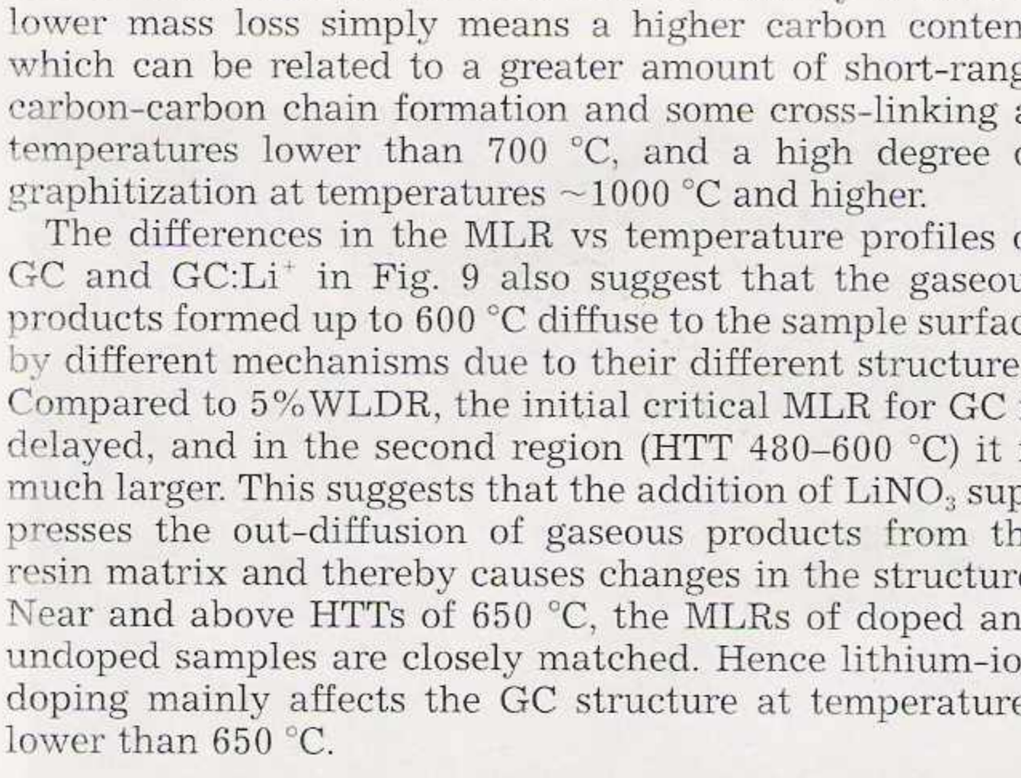

Fig. 9. DTG of cured resol and 5%WLDR. Maximum mass loss rate for the undoped sample is delayed and is higher by 9–10%.

We have previously shown that diffusion of the gaseous products in GC up to 500 °C does not follow Fick's second law (diffusion time proportional to length squared), but between 230 and 330 °C, this diffusion varies with the fifth power of the length and with the third power between 330 and 500 °C.[22] We probed the diffusion mechanism by direct observation of lithium-ion leaching. Figure 10 shows ICP-AES results for the amount of lithium ion leached into PBS from GC:Li^+ electrodes of HTT 500, 575, and 650 °C. The lithium-ion out-diffusion rate from the HTT 650 °C sample is higher than that from the 500 and 575 °C samples. This suggests that the diffusion rate is controlled not only by surface but by the bulk as well. For confirmation of bulk diffusion, scanning electron micrographs from the freshly broken cross section of the samples were made.

Figures 11a-c are scanning electron micrographs showing the pore size distribution of GC:Li^+ samples after heat-treatment at 500, 650, and 1000 °C at a freshly broken cross section. Compared to undoped GC, the pore size of GC:Li^+ samples of intermediate HTTs is smaller. For GC of 500 °C HTT, the mean pore size diameter is ~60 μm; for GC:Li^+, the pore diameter varies between 10 and 15 μm; and for samples of 1000 °C HTT, the pore size for GC is smaller than for GC:Li^+. Differences in MLRs and pore sizes between the doped and undoped GCs may be correlated with the greater differences observed between their electrochemical behavior.

The large difference between OCPs of GC:Li^+ and GC, in the 600–650 °C range, shown in Fig. 7a, may also be attributed to the influence of the different structures evidenced by the different MLRs, pore-size distribution, and the diffusion mechanism. As the HTT increases, more graphene forms and, at the same time, lithium compounds and their derivatives (associated with the endothermic reaction near 700 °C in Fig. 12) escape from the sample. With increasing degree of graphitization, the structural changes caused by lithium doping at lower temperatures are partially reversed, so that the OCP values of GC:Li^+ and GC samples approach closer to each other (Figs. 7a and b). This may be pictured as the formation of carbon-carbon bonds or, perhaps, short-range graphene sheets, in those locations where lithium compounds and derivatives prevent the natural carbon-carbon bonding during the initial increase of temperature.

Analysis of X-ray diffraction profiles.—The structural changes in GC:Li^+ and GC were also determined from X-ray diffraction (XRD) peak profiles[22] produced by a Philips PW-1840 powder diffractometer. As a measure of the graphene layers, we calculated the ratio of the height of the (002) Bragg peak to the background (R) from the

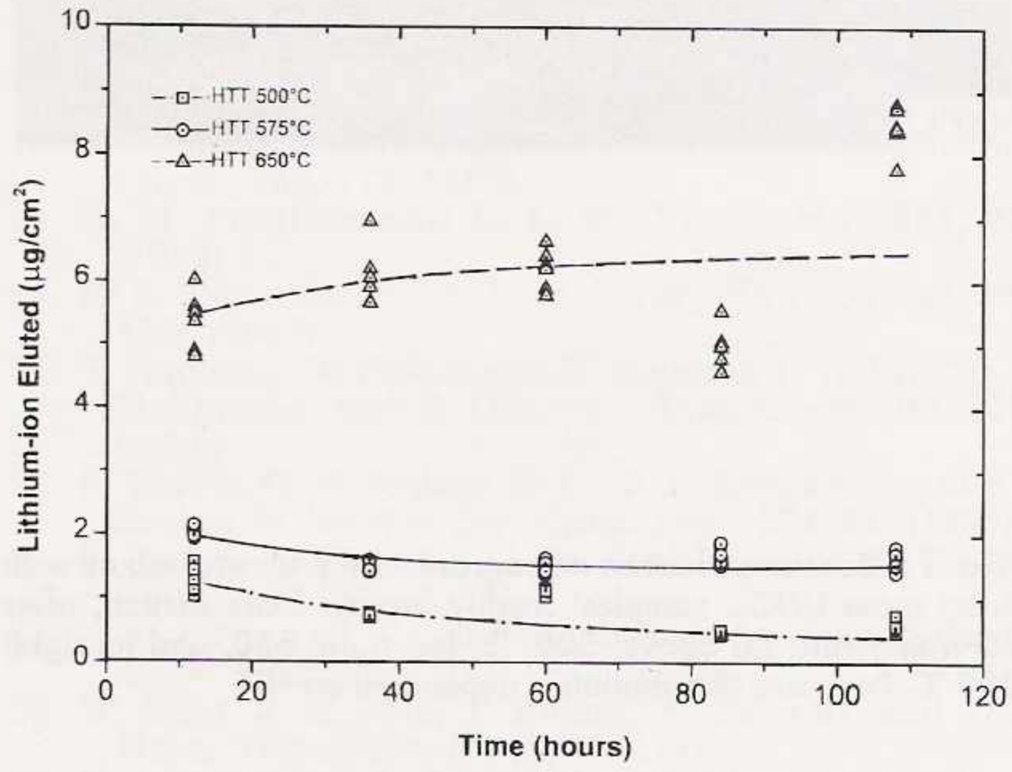

Fig. 10. Plot of lithium ion released into PBS solution from a mixture of resol and 10% by mass lithium nitrate (10%WLDR) heat-treated to 500, 575, and 650 °C, every 24 h for 5 days. Note that the 650 °C sample Li^+ release rate is higher than the other samples. Results shown from five independent experiments for each HTT.

XRD profiles of our samples following a method given elsewhere.[44,42] For a 500 °C HTT, d_{002} = 4.00 Å and R = 1.84 in GC:Li^+ and d_{002} = 3.84 Å and R = 1.78 in GC; for 1000 °C HTT, d_{002} = 3.36 Å and R = 2.33 in GC:Li and d_{002} = 3.61 Å and R = 1.83 in GC. These results show the formation of a large number of dispersed short graphenes in GC:Li of HTTs < 700 °C and an enhanced graphitization in GC:Li with HTT 1000 °C. This may be the cause of the large hysteresis shown by GC:Li^+ of HTTs < 700 °C compared to HTTs of 1000 °C in the CVs of Fig. 8. It appears that an inverse response hysteresis to HTT is characteristic of most of the disordered carbons in an electrochemical system. This behavior is also observed when a heat-treated perylenetetra carboxylic dianhydride of HTT < 700 °C is used as an anode in a lithium-ion battery.[43]

Differential scanning calorimetry.—DSC results for 5%WLDR showed large differences between GC:Li^+ and pure GC (Fig. 12). No endothermic peak was observed for GC similar to that for GC:Li^+ near 720 °C under the same experimental conditions. This is attributed to the melting of LiOH and/or Li_2CO_3, since it occurs close to the melting points of both compounds (680 and 723 °C, respectively). The presence of the endothermic peak near 700 °C and the fact that the XPS result shows zero lithium remaining in GC:Li^+ of HTT 1000 °C suggest the following mechanism.

When $LiNO_3$ is dissolved in a liquid solution of resol, the nitrate ions associate mainly with the alcohol used to control the resin viscosity; the lithium ion associates with oxygen, hydroxyl, and carbonate groups rather than attaching to linear chains and/or cross-linked carbons. It most likely forms Li_2O, LiOH, and Li_2CO_3 during postcuring and precarbonization (HTT ~230–600 °C). This explains the highly pronounced endothermic peak between 680 and 740 °C and suggests the possibility that GC:Li^+ also contains species that are produced by the reaction of molten lithium compounds (mostly LiOH and/or Li_2CO_3, but not necessarily Li_2O because of its high melting point) with gaseous products of carbonization. This and the presence of carbon with hydrogen links can also be reasons for the large hysteresis in the voltammogram of the 700 °C HTT GC:Li^+ sample (Fig. 8), especially because none of the other samples shows such a large hysteresis.

Soon after the temperature exceeds 723 °C, the reactions $Li_2CO_3 \rightarrow Li_2O + CO_2$ and $2LiOH \rightarrow Li_2O + H_2O$ become possible. On further heating to 1000 °C, H_2O, CO_2, and Li_2O diffuse out; the hydrocarbon gas partially reacts with other carbon atoms (e.g., $C_n + CH_4 \rightarrow C{\cdot}C_n + 2H_2$) by pyrodeposition, and the rest diffuses out; the hydrogen produced also diffuses out. Any carbon atoms produced by these reactions bond to the carbon atoms immediately surrounding them, hence the total carbon residue in the bulk of the GC:Li^+ increases. This decreases the H/C and O/C ratios and can consequently change the effects of the basic-carbon surface species such as carbonyl and hydroxyl groups.

In summary, lithium doping results in the formation of a carbonaceous structure with a large amount of short carbon chains which end in hydrogen. This, as well as the structural changes due to a different out-diffusion mechanism of the gaseous products of carbonization compared to that of pure GC, could be the reason for GG:Li^+ exhibiting large hysteresis in electrochemical experiments. The larger double-layer capacitance area of GC:Li^+ of HTT 700 °C (Fig. 8) is indicative of its larger surface area compared to GC:Li^+ of other HTTs.

It appears that the large hysteresis for disordered carbon of HTTs < 1000 °C is correlated with H/C.[44] Mesophase-

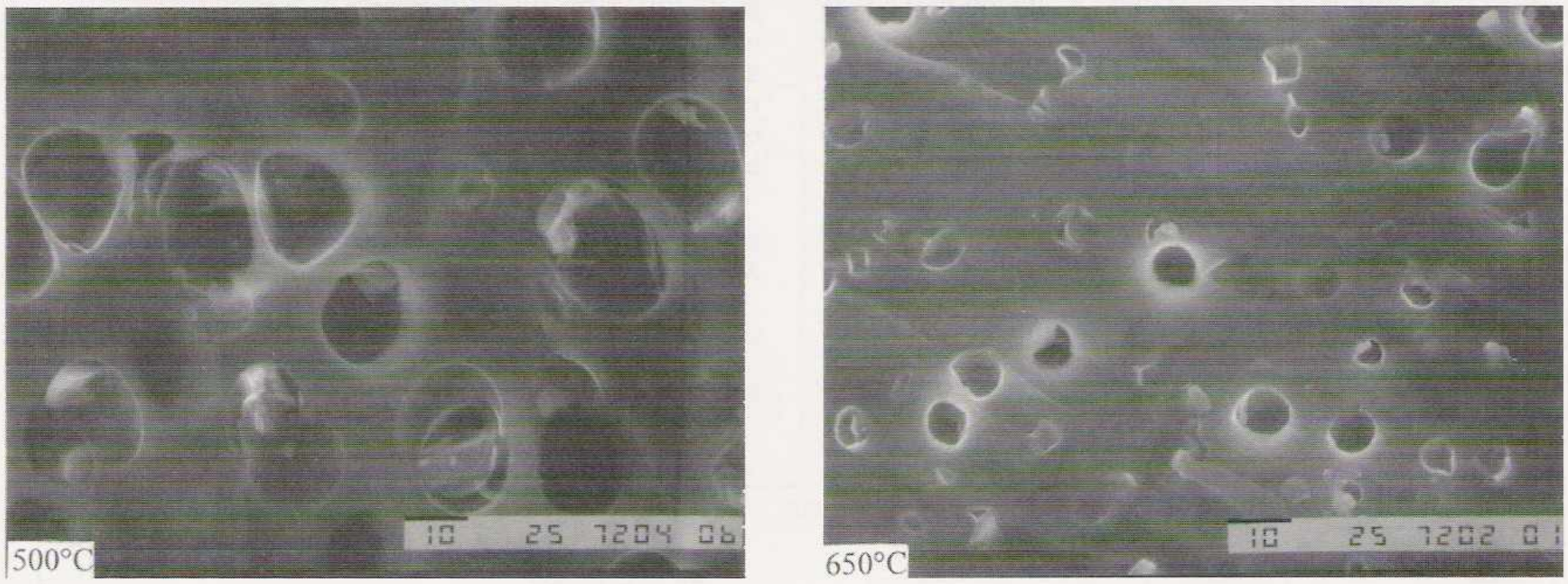

Fig. 11. Scanning electron micrograph of liquid resol mixed with 5% by mass $LiNO_3$; samples' freshly broken cross section, after heat-treatments: (a, above) 500, (b, top right) 650, and (c, right) 1000 °C. Pore-size distribution is dependent on HTT.

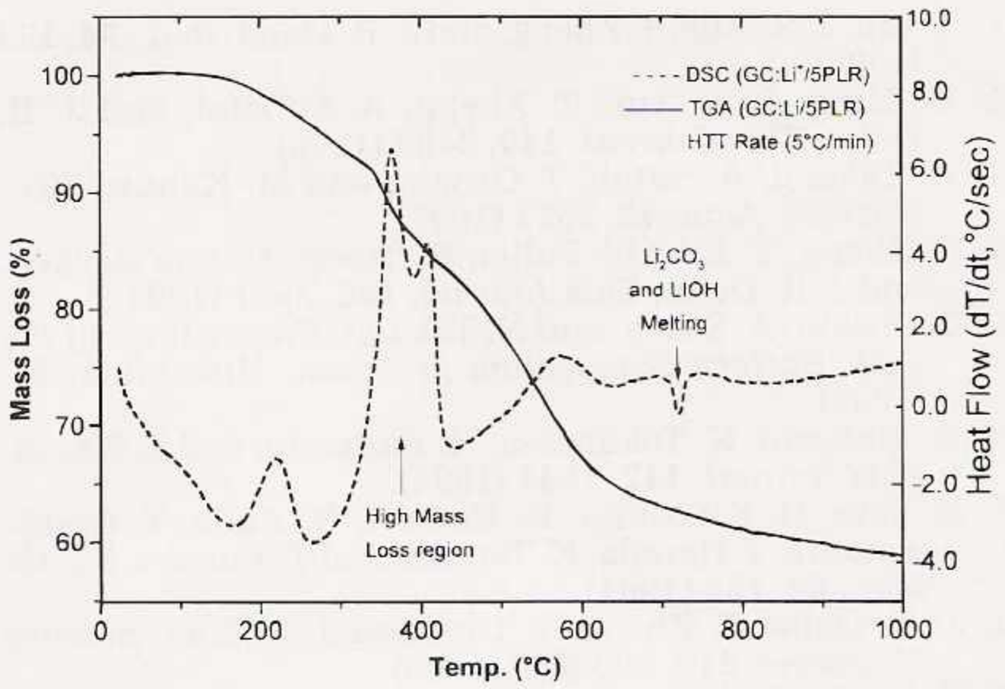

Fig. 12. DTG and DSC showing mass loss and endo/exothermic nature of reaction of species in cured 5%WLDR on heating to 1000 °C. Endothermic reaction between 680 and 740 °C is due to melting of LiOH and Li_2CO_3.

pitch-based carbon[45,46] and phenolic-resin-based GC[47] of HTT < 1000 °C show a high specific capacity with a large hysteresis in potential when used as anode in lithium-ion batteries. Dahn et al.[48] showed that the lithiation capacity of hard carbon anode materials, such as GC or HTT around 700 °C, depends on the H/C ratio. Yata et al.[47] showed that phenolic-resin-based carbons prepared at these temperatures contain a substantial amount of hydrogen. Their materials showed a high lithiation capacity for H/C ratios in the neighborhood of 0.2. Enoki et al.[49] showed that charge transfer from alkali atoms to hydrogen in carbon is expected. Therefore, it is reasonable to believe that lithium atoms bond to carbon in the vicinity of H atoms in hydrogen-containing carboneous material such as GC, if the latter is heat-treated to near 600–700 °C. The inserted lithium transfers part of its 2s electron (in a covalent bond) to a nearby hydrogen, resulting in a corresponding change to the H-C bond. This would cause changes in the relative atomic positions of the C and H atoms to cause hysteresis in electrochemical measurements.[50]

For a high-capacity and/or high-discharge-rate lithium-ion battery, the GC:Li^+ of various HTTs would be an interesting material to investigate, because it can be tailored simply by controlling the additive concentration and heat-treatment program. To obtain dense GC products with the smallest possible pore sizes, it is best to heat-treat precursor material slowly (< 2 °C/h for samples ~1 mm thick) to the precarbonization stage (100–600 °C) and to ensure a long annealing time before critical mass loss is initiated (300 °C in this case). Finally, the concentrations of the added salt and melting/decomposition temperature of its byproducts are also important for tailoring the GC to the desired structure.

Conclusions

The strong influence of HTT on the voltammetric response of GC electrodes, especially with respect to hydrogen evolution, has been demonstrated. The oxidation of electroactive species at low positive potentials up to 1 V vs SCE is not significantly affected by the HTT because this occurs in a relatively unreactive region of potential. However, as for other GCs, the electrode pretreatment and history can markedly influence the electrode kinetics. For voltammetric applications, samples heat-treated to above 2000 °C are clearly the most appropriate because electrolyte background currents are lowest over the widest potential ranges.

Lithium-ion doping causes changes in properties and structure of the GC, as evidenced by electrochemical and DTG results of this work and XRD from previous work. Although ICP-AES results show that the lithium ions have been expelled from the heat-treated resins and XPS data show that no lithium ions remain in samples of HTT 1000 °C and higher, the structure remains altered. Thus, this is a route to permanently altering the GC structure. We are currently analyzing this further by using the dopants $Mg(NO_3)_2$, $Al(NO_3)_3$, and H_3BO_3.

Acknowledgments

This project was supported by the National Science Foundation EPSCoR-II, under grant no. EHR-9108761, to the Howard J. Foster Center for Irradiation of Materials at Alabama A&M University, and by the U.S. Army Office (ARO) under grant no. DAAH04-94G-0055; to Illinois Institute of Technology. Financial support to C. D. Cojocaru under the European Community Tempus Program (JEP-04223-95/3) is acknowledged. The authors thank A. P. Piedade, Coimbra University, for EPMA work, and L. Allerd and W. Porter at HTML, Oak Ridge National Lab, for TEM and STA works, respectively (contract no. DE-A05-96OR22464). Georgia-Pacific, Atlanta, GA, supplied the resin precursor.

Manuscript submitted May 12, 1997; revised manuscript received November 14, 1997.

Alabama A&M University assisted in meeting the publication costs of this article.

REFERENCES

1. G. M. Jenkins and K. Kawamura, *Polymeric Carbons-Carbon Fiber, Glass and Char*, Cambridge University Press (1976), currently being updated for publication in 1997.
2. R. L. McCreery, in *Electroanalytical Chemistry*, Vol. 17, A. J. Bard, Editor, p 271, Marcel Dekker, New York (1991).
3. C. M. A. Brett and A. M. Oliveira Brett, *Electrochemistry Principles, Methods, and Applications*, pp 130-133, Oxford University Press, Oxford (1993).
4. W. E. van der Linden and J. W. Dieker, *Anal. Chem. Acta*, **119**, 1 (1980).
5. H. E. Zittel and F. J. Miller, *Anal. Chem.*, **37**, 200 (1965).
6. R. J. Rice, N. M. Pontikos, and R. L. McCreery, *J. Phys. Chem.*, **112**, 4617 (1990).
7. D. C. Thornton, K. T. Corby, V. A. Spendel, J. Jordan, A. Robbat, Jr., D. J. Rutstrom, M. Gross, and G. Ritzler, *Anal. Chem.*, **57**, 150 (1985).
8. G. N. Kamau, W. S. Willis, and J. F. Rusling, *ibid.*, **57**, 545 (1985).
9. I. F. Hu, D. Karweik, and T. Kuwana, *J. Electroanal. Chem.*, **188**, 59 (1985).
10. P. Heiduschka, A. W. Munz, and W. Göpel, *Electrochim. Acta*, **39**, 2207 (1994).
11. R. C. Engstrom, *Anal. Chem.*, **54**, 2310 (1982).
12. R. C. Engstrom and V. A. Strasser, *ibid.*, **56**, 136 (1984).
13. T. Nagaoka and T. Yoshino, *ibid.*, **58**, 1037 (1986).
14. J. Mattusch, K.-H. Hallmeier, K. Stulík, and V. Pacáková, *Electroanalysis*, **1**, 405 (1989).
15. A. L. Beilby, T. A. Sasaki, and H. M. Stern, *Anal. Chem.*, **67**, 976 (1995).
16. C. Barbero and R. Kötz, *This Journal*, **140**, 1 (1993).
17. H. Zhang and L. A. Coury, Jr., *Anal. Chem.*, **65**, 1552 (1993).
18. K. Stulik, D. Brabcova, and L. Kavan, *J. Electroanal. Chem.*, **250**, 173 (1988).
19. N. M. Pontikos and R. L. McCreery, *ibid.*, **324**, 229 (1992).
20. R. K. Jaworski and R. L. McCreery, *This Journal*, **140**, 1360 (1993).
21. T. Nagaoka, T. Fukunaga, T. Yoshino, I. Watanabe, T. Nakayama, and S. Okazaki, *Anal. Chem.*, **60**, 2766 (1988).
22. H. Maleki, G. M. Jenkins, D. Ila, R. L. Zimmerman, and L. Evelyn, *Mater. Res. Soc. Symp. Proc.*, **371**, 443 (1995).
23. J. Fisher, L. Holland, G. M. Jenkins, and H. Maleki, *Carbon*, **34**, 789 (1996).
24. A. L. Evelyn, D. Ila, and G. M. Jenkins, *Nucl. Instrum. Meth. Phys. Res.*, **B85**, 861 (1994).
25. W. Xing, J. S. Xue, T. Zheng, A. Gibaud, and J. R. Dahn, *This Journal*, **143**, 3482 (1996).
26. R. J. Taylor and A. A. Humffray, *J. Electroanal. Chem.*, **43**, 347 (1973).
27. M. Noel and P. N. Anantharaman, *Analyst*, **110**, 1095 (1985).
28. P. Chen, M. A. Fryling, and R. L. McCreery, *Anal. Chem.*, **67**, 3115 (1995).

29. K. Takahashi, K. Yoshida, and M. Iwaki, *Electrochim. Acta*, **35**, 1279 (1990).
30. H. Maleki, L. R. Holland, G. M. Jenkins, R. L. Zimmerman, and W. Porter, *J. Mater. Res.*, **11**, 2368 (1996).
31. C. Barbero, J. J. Silber, and L. Sereno, *J. Electroanal. Chem.*, **248**, 321 (1992).
32. A. L. Beilby, T. A. Sasaki, and H. M. Stern, *Anal. Chem.*, **67**, 976 (1995).
33. J. J. O'Dea, J. Osteryoung, and T. Lane, *J. Phys. Chem.*, **90**, 2761 (1986).
34. J. Osteryoung, *Acc. Chem. Res.*, **26**, 77 (1993).
35. C. M. A. Brett, A. M. Oliveira Brett, A. C. Fisher, and R. G. Compton, *J. Electroanal. Chem.*, **334**, 57 (1992).
36. K. Kinoshita, *Carbon Electrochemical and Physicochemical Properties*, Wiley-Interscience, New York (1988).
37. J. F. Evans and T. Kuwana, *Anal. Chem.*, **49**, 1632 (1977).
38. D. C. S. Tse and T. Kuwana, *ibid.*, **50**, 1315 (1978).
39. H. Xiang, S. Fang, and Y. Jiang, *This Journal*, **144**, L187 (1997).
40. Y. Yamashita and K. Ouchi, *Carbon*, **19**, 89 (1981).
41. Y. Liu, J. S. Xue, T. Zheng, and J. R. Dahn, *ibid.*, **34**, 193 (1996).
42. W. Xing, J. S. Xue, T. Zheng, A. Gibaud, and J. R. Dahn, *This Journal*, **143**, 3482 (1996).
43. N. Takami, A. Satoh, T. Ohsaki, and M. Kanda, *Electrochim. Acta*, **42**, 2537 (1997).
44. T. Zheng, Y. Liu, W. Fuller, S. Tseng, U. von Sacken, and J. R. Dahn, *This Journal*, **142**, 2581 (1995).
45. T. Ohsaki, A. Satoh, and N. Takami, *Proceedings of the 34th Battery Symposium in Japan*, Hiroshima, 79, (1993).
46. A. Mabushi, K. Tokumitsa, H. Fujimoto, and T. Kasuh, *This Journal*, **142**, 1041 (1994).
47. S. Yata, H. Kinoshita, K. Komori, N. Ando, T. Kashiwamura, T. Harada, K. Tanaka, and T. Yamabe, *Synth. Met.*, **62**, 153 (1994).
48. J. R. Dahn, T. Zheng, Y. Liu, and J. S. Xue, *Science Magazine*, **270**, 590 (Oct. 1995).
49. T. Enoki, S. Miyajima, M. Sano, and H. Inokuchi, *J. Mater. Res.*, **5**, 435 (1990).
50. L. S. Selwyn, W. R. McKinnon, U. von Sacken, and C. A. Jones, *Solid State Ionics*, **22**, 337 (1987).